Available online at www.sciencedirect.com

SciVerse ScienceDirect

journal homepage: www.elsevier.com/locate/issn/15375110

Research Paper

Novel image processing approach for solving the overlapping problem in agriculture

*Julio C. Pastrana**, *Thomas Rath*

Leibniz Universität Hannover, Institute of Biological Production Systems, Biosystems and Horticultural Engineering Section, Herrenhäuser Str. 2, 30419 Hannover, Germany

ARTICLE INFO

Article history:
Received 27 June 2012
Received in revised form
30 November 2012
Accepted 7 December 2012
Published online 27 March 2013

A general problem in computer vision is the detection of objects when they are partially occluded. This problem also extends to the identification of horticultural/agricultural products (e.g., plants and crops), where recognition can be very cumbersome due to the heavy overlapping situations that one can find. This paper presents a novel approach to solve the recognition of plantlets under such conditions. The methodology consists of two major steps: (1) The simplification of the complexity of leaf shapes by using ellipse approximation. (2) The clustering of the leaves (ellipses) found into plantlets using active shape models. Shape models of experimental plants with 2, 3 and 4 leaves were tested to analyse the ability of the method to overcome the overlapping problem. The results indicate that the presented technique is able to perform identification of individual plantlets under overlapping situations, by first decreasing the complexity of their form and then using these simplified characteristics in a statistical shape model.

1. Introduction and objectives

Image processing is a basic tool in agriculture. It is used for automation and robotics, for phenotyping, sorting and a lot of different measurements in science and practice. Currently, there are many image processing techniques that only take into account the colour information provided by the captured images to perform object detection. Normally they use colour segmentation to separate regions of interest (RoI) – in the case of plant applications, the green of the plants – in order to identify the areas that might have some information useful for the vision recognition system. There are different methods to perform the segmentation process, just to mention some: histogram thresholding, feature space clustering, region based edge detection, fuzzy logic, neural network approaches, etc. Each strategy has its pros and cons, and depending on the characteristics of the problem, one has to adopt the most suitable method (Cheng, Jiang, Sun, & Wang, 2001). After identifying the region(s) that might contain the object(s) that one is looking for, it is necessary to search for patterns that would lead to the proper identification of the objects. This pattern recognition is challenged by the fact that the objects that one wants to recognise are normally overlapped by other objects. This means that the identified RoIs contain information that is incomplete, and somehow the selected pattern recognition technique has to find the way to work around missing features and still be able to recognise the desired object(s). For example, Hemming and Rath (2001), in their attempt to differentiate between crops and weeds in open field situations, used geometric primitives to differentiate between plant

* *Corresponding author.*
E-mail addresses: pastrana@bgt.uni-hannover.de, juliopastrana@yahoo.com (J.C. Pastrana), rath@bgt.uni-hannover.de (T. Rath).
1537-5110/$ – see front matter
http://dx.doi.org/10.1016/j.biosystemseng.2012.12.006

Nomenclature

ASM	active shape models
α	arc detection variable
(x, y)	Cartesian coordinates
$(\overline{x}, \overline{y})$	centroid or centre of gravity
cp	closest perimeter point
i,j,n,m,q	counters
de	deformation energy
b	deformation values
ec	ellipse centre
NIA	ellipse new information area
EOA	ellipse overlapping area
EPA	ellipse pixel area
λ	eigenvalue matrix
Φ	eigenvector matrix
I	image
IEF	identification effectiveness
s	landmarked shape
w_a and w_b	leaf width
μ	mean value
$\boldsymbol{\mu}$	mean shape matrix
θ	radial angle
r	radial distance
RoI	region of interest
$\mathbf{p}^i = (p^i_R, p^i_G, p^i_B)$	RGB pixel
S	set of shapes
thr	threshold
pc	virtual plant centre
w_f	weighting factor

types. Nevertheless, the performance of his approach was compromised when plants overlapped each other.

When looking at harvesting robots, e.g., strawberry (Hayashi et al., 2010), cucumbers (Van Henten et al., 2003), etc., there is a common problem: fruits or flowers partially occluded. This means that there are cases when the objects are not recognised, because there is missing visual information. Other examples include the inspection and grading of agricultural products. Brosnan and Sun (2002) mention that it is possible to improve the quality of foods, fruits, vegetables and grains by means of vision systems that grade the agricultural products but nonetheless, all the methods mentioned in their review also have the problem that in order to cope with the production necessities, they have to be less sensitive to partly occluded objects. One can state that the overlapping problem is one of the basic problems of all biorobotic systems, and currently has not been solved.

Therefore the objective of this investigation was to develop a vision system to overcome the overlapping problem in plant applications.

2. Materials and methods

2.1. General idea of the algorithm

The overlapping problem was faced by developing special image processing algorithms which can be encapsulated in 4 general steps:

1. Region of interest (RoI) analysis using colour segmentation
2. Leaf detection using ellipses
3. Data compression using ellipse landmarking
4. Pattern recognition using an active shape model (ASM) approach.

The implemented algorithms were tested using different scenes of overlapping seedlings, which were scattered in different arrangements in order to create variability. Additionally, artificially generated overlapping situations were also used to test the ability of the method to solve problems ranging from slight to heavy overlapping.

2.2. Plants and growing conditions

For model development and evaluation of the methods, the plant *Nicotiana tabacum* was selected. This species was chosen because the plantlets are fast growing and have more or less uniform growth characteristics. The plants were sown in trays measuring 20 cm by 15 cm. Scenes were generated using plants with non-overlapping conditions, for example, they were sown in rows of 3 by 3. Other trays were prepared with the seeds planted closer together, for instance in rows of 7 by 5 plants or in random patterns, in order to create overlapping. The plantlets were grown in a greenhouse with a temperature of 23 ± 2 °C, in a peat-based substrate, without the use of pesticides.

2.2.1. Scenes with natural overlapping situations

A series of images were taken over a period of two weeks after germination. A total of 6 cases, with different planting arrangements were created (see Table 1). Figure 1 presents 3 of the previously mentioned cases.

2.2.2. Scenes with artificially generated overlapping situations

Several case studies were analysed, using images sets with groups of plantlets with 0%, 0.5%, 1%, 2%, 4%, 8%, 16%, and 32% of overlapping area. These image sets were generated artificially using image processing software that allowed different pictures of plantlets to be taken, stored in a database

Table 1 – Description of the scenes with *Nicotiana tabacum* seedlings.

Case	Arrangement columns × rows	No. of plants
R_A	5 × 5	32
R_B	6 × 6	36
R_C	6 × 4	21
R_D	5 × 6	28
Rnd_1	random	17
Rnd_2	random	31

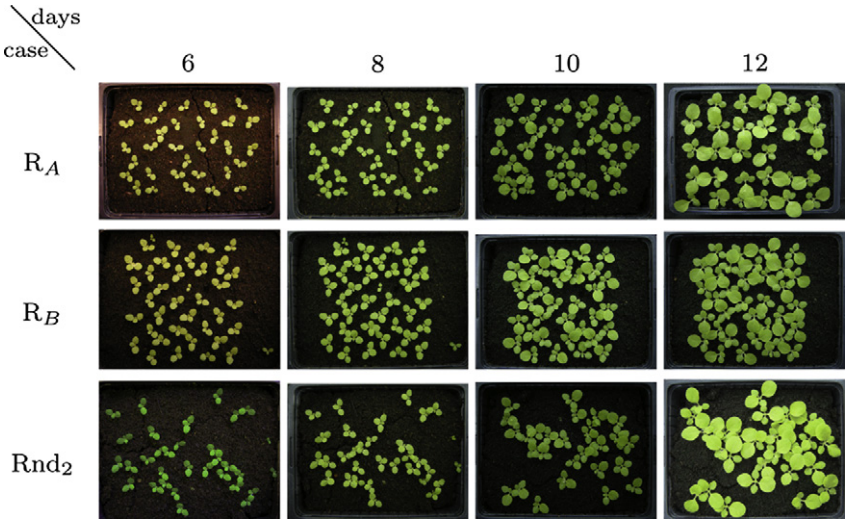

Fig. 1 – Example of scenes showing images with plants over time.

and then combined to create different groups with a similar amount of overlapping area. To create an overlapping group of plants, first the total pixel area of the non-overlapping plantlets that will form the set is computed. Then the plantlets were positioned so that desired percentage of the total pixel area is occluded. This overlapping has to be spread over all the members of the group, i.e., each plantlet has to be overlapped by at least one other, but not necessarily by the same amount. Every overlapping scene is composed of 8 images.

2.3. *Image acquisition and segmentation*

The image acquisition was done with a stand and a commercial camera (Nikon Coolpix P5000). In this way, series of photos were always taken from the same position, i.e. directly above the plantlet tray. After germination, the plantlets were photographed every day over a period of 2 weeks in a phytochamber with constant light conditions.

In order to separate the soil from the plants, an enhancement step and a colour filter were used. This method is an adaptation from the excess green index technique proposed by Woebbecke, Meyer, von Bargen, and Mortensen (1995). Finally, a threshold only allows regions of the green channel to pass through the filter. Details of the segmentation procedure of an input image I with n pixels $\mathbf{p}^i = (p_R^i, p_G^i, p_B^i)$ are below.

Compute the minimum and maximum of the green enhanced values.

$$\min p_G = \min_{1\le i\le n}\left[(p_G^i - p_R^i) + (p_G^i - p_B^i)\right]$$

$$\max p_G = \max_{1\le i\le n}\left[(p_G^i - p_R^i) + (p_G^i - p_B^i)\right]$$

Establish the mean μ of the green enhanced values with the help of a weighting factor w_f within the interval (0,1). The value of this factor will determine how strict the threshold thr will be. During the experimental phase the value of w_f was set to 0.5.

$$\mu = (\max p_G + \min p_G)\cdot w_f$$

$$thr = \frac{\mu - \min p_G}{\max p_G - \min p_G}\cdot 255$$

Then, for all pixels p^i, where $(1 \le i \le n)$, compute the new values p_G^* of the green channel and binarise using the previously calculated threshold.

$$p_G^* = \frac{p_G^i - \min p_G}{\max p_G - \min p_G}\cdot 255$$

$$p_G^i = \begin{cases} 1 & \text{if } p_G^* \ge thr \\ 0 & \text{if } p_G^* < thr \end{cases}$$
$$p_R^i = p_B^i = 0$$

After binarisation, a border extraction algorithm proposed by Suzuki and Abe (1985) was used to extract the outlines. This algorithm performs a topological analysis to produce a collection of contours and store them in a hierarchical tree data structure.

2.4. *Leaf identification by ellipse detection using arcs*

The presented work is concerned with plants that are composed of a set of leaves where a single leaf has, to a certain degree, an elliptical form.

There are several ways in which the task of ellipse detection in binary images can be carried out. For instance, Yuen, Illingworth, and Kittler (1989) and Mclaughlin (1998) proposed similar techniques based on the Hough transform and the random selection of 3 points along the outline of the shape to generate possible ellipses. All these methods use a voting scheme to find the ellipses, in which small ellipses have a very small chance of being detected because larger ellipses have a higher probability that their points will be selected to generate possible ellipses. Therefore, a new ellipse detection method was developed: the methodology is based on the detection of arc-sections within the outline of a given region. The identified arc-sections are then combined in order to fit ellipses that best superimpose the region that is being analysed.

Fig. 2 – Example scenes of artificially generated overlapping.

If one uses the (r,θ) signature (Zhang & Lu, 2004) to represent ellipses, it is possible to visualise that they have variable radial distance to the centre, always varying between the value of the semi-major axis and the semi-minor axis. In this research, a special signature that takes advantage of the previously mentioned behaviour is used to calculate the different arc sections of a shape contour. This signature can be calculated in the following manner:

Having an n number of (x, y) points on the shape boundary, one starts by calculating the centroid $(\bar{x}, \bar{y})$

$$\bar{x} = \frac{1}{n}\sum_{i=1}^{n} x_i, \quad \bar{y} = \frac{1}{n}\sum_{i=1}^{n} y_i \tag{1}$$

the radial distance r_i from each point to the centroid is

$$r_i = \sqrt{(x_i - \bar{x})^2 + (y_i - \bar{y})^2} \tag{2}$$

and the corresponding radial angle is

$$\theta_i = \arctan\frac{y_i - \bar{y}}{x_i - \bar{x}} \tag{3}$$

The θ_i values are always increasing or decreasing in the form of a *wave*. The grouping of points, which form an arc can be done by following negative or positive changes and stopping when the change becomes zero or positive or negative. However, in the case of circles the (r,θ)signature is a line and the analysis of the ascending or descending values of θ is not possible, see Fig. 3.

In order to carry out such an analysis, a new variable α was incorporated into the calculations using the r_i and θ_i values, see Fig. 4.

$$\alpha_i = r_i \sin(\theta_i)\cos(\theta_i) \quad \text{where} \quad 1 \le i \le n \tag{4}$$

The developed algorithm enables the detection of arcs in a binary image by analysing the border pixels of the binary shapes. It starts with the calculation of the centre of gravity of the shape, then calculating r_i, θ_i and α_i, for further analysis of the α_i changes. If a change occurred, the so far analysed boundary pixels are stored as an arc in a database. The rest of the contour pixels are analysed in the same way until the whole outline is evaluated. The resulting arcs are sorted according to length in order to identify which arcs provide the greatest amount of information about the shape (long arcs give more information about the outline). Finally, the algorithm applies a threshold that removes arc sections that are too small and can be considered negligible. Figure 5 depicts the result after applying the arc detection algorithm to a plant contour.

The next step in the ellipse identification process is to combine neighbouring arc sections to approximate the ellipse that best represents the area in which the arcs are situated. In order to carry out the combination, the middle point (point located in the middle of the arc sequence) of each arc section must be found. The arcs with the greatest number of points were selected first. Then, by using the Euclidean distance between the arc middle points, the $m = 25$ nearest arc neighbours (25 was chosen to avoid over-estimation), where the line segment connecting their middle points are fully contained in the shape area were selected. Whenever a couple of pixels of the line segment are outside the region of interest, the arc sections are not recognised as neighbours (see Fig. 6).

After finding the arc neighbours of a given arc section, the algorithm starts combining them in order to find the ellipse that best fits the area (RoI) where the arcs are found. Each arc combination has to fulfil the conditions presented in Eq. (5).

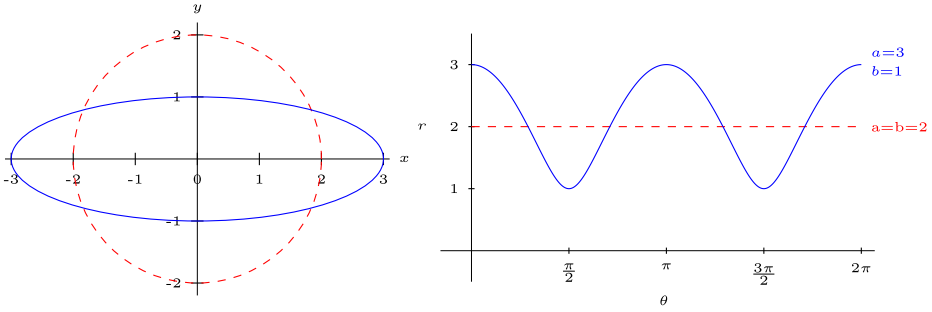

Fig. 3 – Behaviour of the (r,θ) signature using an ellipse and a circle with major axis a and minor axis b. r is radial the distance to the centre and θ is the angular coordinate.

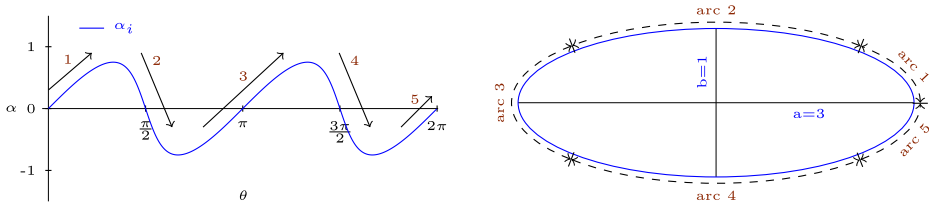

Fig. 4 – Ellipse arc-extraction using ascending descending analysis of the α_i values. Left side image shows a line that corresponds to the computed α_i values after the analysis of the outline. Right side image shows the input ellipse and detected arcs.

$$\begin{array}{ll} EOA = numpix(EPA \cap RoI) & EOA \geq EPA \times 0.97 \\ NIA = unoccpix(EPA) & NIA \geq EPA \times 0.20 \end{array} \quad (5)$$

where *EOA* is the ellipse overlapping area, *NIA* is the new information area, *numpix* is the number of pixels, *unoccpix* are pixels not marked as occupied area, *RoI* is the area to be analysed, and *EPA* is the overall pixel area of the tested ellipse (see Fig. 7).

Fig. 7 depicts an example of two ellipses that are being analysed to determine if they provide enough information to be considered possible leaves. In this case ellipse *A* was first detected. Therefore, it is considered a valid leaf and it is marked as occupied. Then, a new ellipse *B* tries to compete for the area that already belongs to ellipse *A*. This means that the new information *NIA* provided by *B* has to be greater or equal than $0.2 \times EOA$ to be considered a valid leaf.

If the thresholds were not fulfilled, then a new combination with another neighbouring arc has to be tested. This procedure has to be repeated until all arcs of the list are evaluated. One should note that if a single arc provides enough information, it also can be used to approximate a possible ellipse.

Since the list that contained the arcs was sorted according to length, the procedure starts with the combinations with maximum density, thus ensuring that the best ellipses will occupy its corresponding area at the beginning of the process and make the other ellipses with less density compete for a part of the surface within the region of interest. At the end of this process, a list of more or less overlapping areas which represent leaves is available. The next step is to combine these ellipses into plants.

2.5. *Data compression using landmarking of ellipses*

In order to analyse and calculate shapes, it is essential to reduce the boundary to specific points (landmarks), which will represent the shape. For this, different algorithms could be used. They are based on fixed points of shapes or on general procedures to find edges in shapes.

The proposed landmarking procedure belongs to the first group. It computes 5 points for each detected ellipse and 1 extra point for the centre of the plant. The plant centre is only used as the anchor point to shift the plant to the origin. The landmarks are given by (see Fig. 8):

1. The ellipse centre (centre of gravity of the ellipse) (*ec*).
2. The closest perimeter points of combined ellipses (*cp*).
3. The virtual plant centre (mean point between the *cp* points of the combined ellipses) (*pc*).
4. The furthest point to the virtual plant centre on the ellipse (*fp*).
5. The two points (w_a and w_b) that maximise the orthogonal distance to the line segment created by *cp* to *fp*.

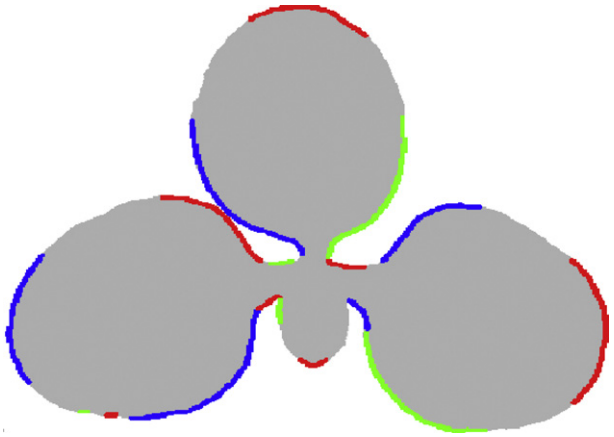

Fig. 5 – Arc extraction on a real plant contour. This example image only shows the arc sections composed of more than 20 pixels.

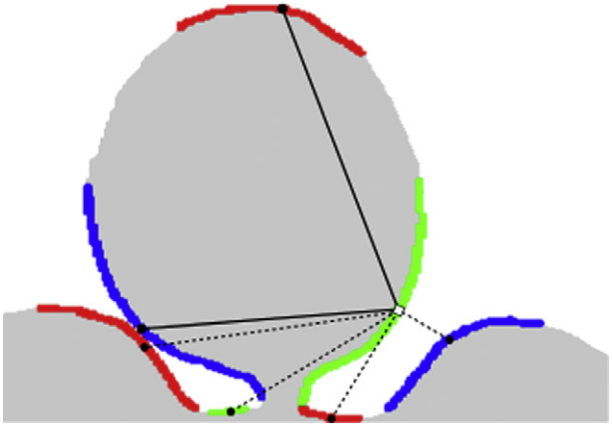

Fig. 6 – Identifying real arc neighbours. Drawing lines on the RoI: Solid lines identify real neighbours, whereas dashed lines identify spurious neighbours.

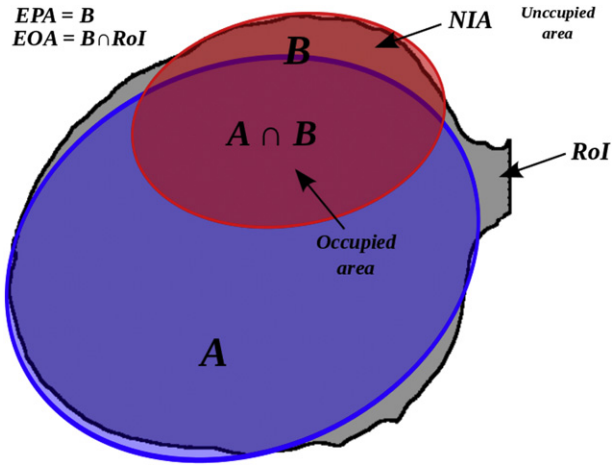

Fig. 7 – Ellipse validation: This image shows two ellipses A and B, in which ellipse A is already a detected leaf and ellipse B is being analysed to see if it can be considered a leaf.

After finding the landmarks, their normalisation and rotation is carried out to eliminate the scale and rotation variances.

2.6. *Pattern recognition using an active shape model approach*

Active shape models incorporate statistical information obtained from a learning set into model templates. These templates have the capability of being altered to create new shapes which are similar to the ones included in the original learning set, thus, allowing the models to be applied in different circumstances (Cootes, Taylor, Cooper, & Graham, 1995).

Shapes can be represented as a set of n points $p = (x, y) \in \mathbb{R}^2$. Furthermore, a landmarked shape can be represented with the k most representative landmark points. When all landmarks that belong to a specific *shape* $\mathbf{s}$ are assembled as a vector, it is expressed as

$$\mathbf{s} = \{p_1, p_2, p_3, \ldots, p_k\} \tag{6}$$

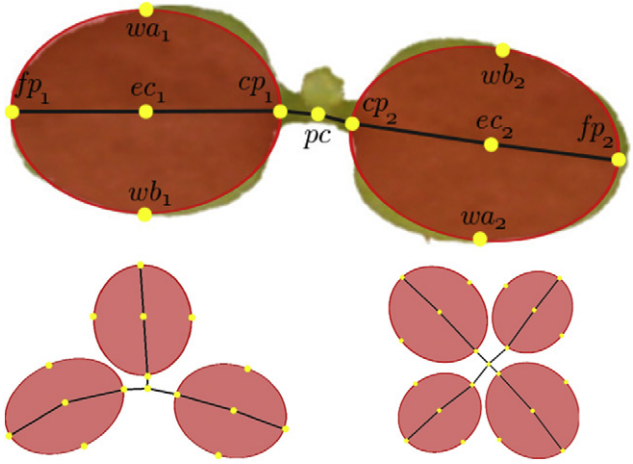

Fig. 8 – Examples of fully landmarked plants.

Thus, a given *set of shapes* $\mathbf{S}_v$ that includes m single shapes is denoted as

$$\mathbf{S}_v = \{\mathbf{s}_1, \mathbf{s}_2, \mathbf{s}_3, \ldots, \mathbf{s}_m\} \tag{7}$$

with a mean shape

$$\boldsymbol{\mu}_v = \frac{1}{m}\sum_{i=1}^{m}\mathbf{s}_i \tag{8}$$

Using a principal component analysis, the main components of the set $\mathbf{S}_v$ are calculated, where the eigenvector matrix $\boldsymbol{\Phi}_v$ and eigenvalue matrix $\boldsymbol{\lambda}_v$ can be used to approximate each element of the set $\mathbf{S}_v$.

Then, each shape $\mathbf{s}$ in the training data set can be approximated by a deformation of the mean shape $\boldsymbol{\mu}_v$ with

$$\mathbf{s} \approx \boldsymbol{\mu}_v + \boldsymbol{\Phi}_v \mathbf{b}_v \tag{9}$$

To ensure that the deformation of the mean shape produces a valid shape, the deformation parameters in b_v have to be bounded by

$$-3\sqrt{\lambda_i} \leq b_i \leq +3\sqrt{\lambda_i} \tag{10}$$

The vector $\mathbf{b} = \{b_1, b_2, \ldots, b_k\}$ deforms the mean shape, and can computed as follows

$$\mathbf{b}_v = \boldsymbol{\Phi}_v^T(\mathbf{s} - \boldsymbol{\mu}_v) \tag{11}$$

Detailed information about the ASM procedures are given in Cootes et al. (1995).

In order to use ASMs for solving the overlapping problem in plant science 210 images of non-overlapping plants with 2, 3 and 4 leaves were used (70 each) to generate 3 deformable templates $(\boldsymbol{\mu}_2, \boldsymbol{\mu}_3, \boldsymbol{\mu}_4)$. The corresponding eigenvectors and eigenvalues were chosen in a way that 99.9% of the total variance of all the landmarked shapes was explained. Figure 9 shows one of the 3 resulting templates.

To analyse an unknown scene with overlapping plantlets, first an image has to be taken from the scene, then, after preprocessing the picture, all possible ellipses are detected

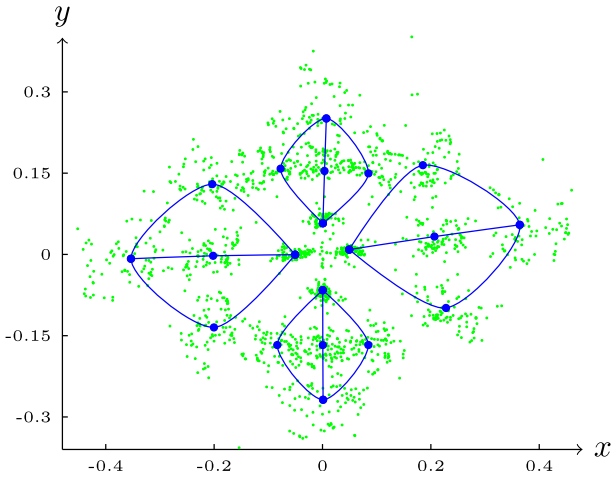

Fig. 9 – Deformable template for *Nicotiana tabacum* plants with 4 leaves. Each green point represents an individual landmark from the training set, the blue points and lines represent the deformable template or mean shape μ_4.

and stored in a list. The pattern matching is done using the following 4 steps:

1. Choose one ellipse of the list and find the 10 closest neighbouring ellipses.
2. Create all possible 2, 3 and 4 leaf plants by combining the 11 ellipses. Naturally, each combination implies finding the landmarks to create a plant. Delete the combinations where the plant centre (using the 3 × 3 pixel square) is not within the original shape.
3. Test the viability of all resulting combinations. This is done by deforming the corresponding mean shape $(\boldsymbol{\mu}_2, \boldsymbol{\mu}_3, \boldsymbol{\mu}_4)$ into the tested plant.
4. The ellipse combination that has the minimum deformation energy *de*, calculated with

$$de = \sum_{i=1}^{n} |b_i| \tag{12}$$

is chosen.

In the case when the ASMs for 2, 3 and 4 leaves are being used simultaneously, a weighting factor is applied. This factor is computed as follows

$$de_{new} = \frac{1}{q} e^{-de} \tag{13}$$

where q is the number of leaves that each plant has.

Finally, the plant to select would be the one with the minimum de_{new}. Clearly, this weighting scheme favours the plants with more leaves; this was done in order to give preference to the more complex shapes that require more deformation energy.

2.7. *Efficiency evaluation of the algorithms*

To get comparable and detailed results an evaluation scheme was developed, which is based on the following scoring system.

1. For every plant correctly detected, one point was awarded for every leaf.
2. For leaf recognition, if they were not used in the formation of a plant, no point was awarded nor deducted.
3. For leaf recognition, if the detection of the leaves of a plant was right, but they were associated to a spurious plant, each leaf properly allocated was assigned with a point, each faulty leaf deducted a point.
4. If a leaf was detected with more than one ellipse, and faulty plants were assigned to these ellipses, for each wrong leaf a point was deducted.
5. The calculation of the identification effectiveness *IEF* was done with

$$IEF = \frac{\text{total points}}{\text{total number leaves}} \times 100\ (\%) \tag{14}$$

3. Results

3.1. *Results using real situations*

Fig. 10 shows the identification result in each of the 6 cases introduced in Table 1.

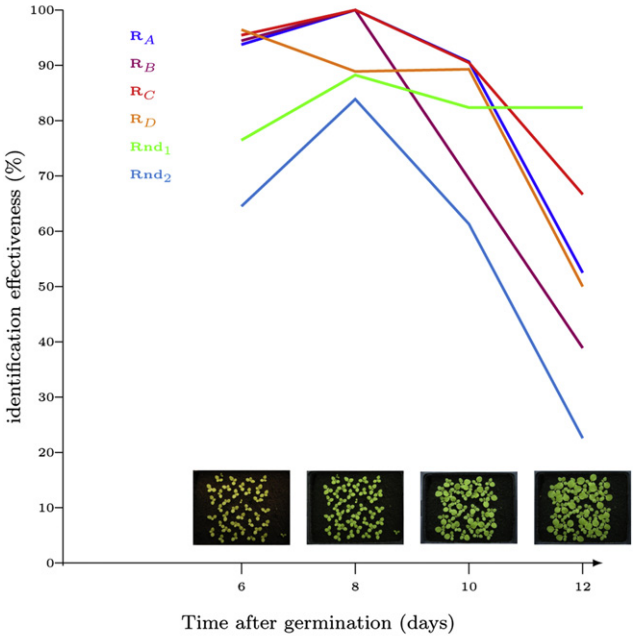

Fig. 10 – Plant recognition in natural scenes. The small images are examples of the growing stages.

From the above plot, one can see that the performance of the detection algorithm increases until the 8th day. This effect is caused by the progressive growing of the plants, leading to a better resolution in the image. Best results were reached around the 8th day, where the resolution is high and the overlapping is low. Despite the fact that after 8 days the edges of the leaves are touching each other, the algorithm is able to reach in some cases 100% effectiveness. Looking at the different scenarios, it is clear that the algorithm has some difficulty with random plant arrangements, especially with a large number of plants (see case Rnd_2 in Fig. 10). Naturally, the plants keep growing (days 10–12), and likewise the overlapping area between the plants. This of course detrimentally affects the accuracy of the detection method, which in some cases decreases its performance to 21% effectiveness.

3.2. *Results using artificially generated situations*

To evaluate the algorithms with fixed and known overlapping, artificial situations were generated (see Section 2). Figure 11 depicts the results. As one can see, with no overlapping, the method is able to detect plants with 2, 3 and 4 leaves with almost 100% accuracy. However, with increasing overlapping, the performance of the method decreases to ca. 21% effectiveness if 32% of the area is overlapped. The greatest amount of difficulty was encountered when analysing overlapping plantlets in one large group. This is because there is a greater number of leaf combinations that can lead to the identification of faulty plants (see Fig. 2 with 32% of overlapping area). To interpret these results, one has to consider that an overlapping of 50% means that two equal shapes are totally on top of each other and no method is able to separate this type of occlusion. Under natural conditions, plants differ from one

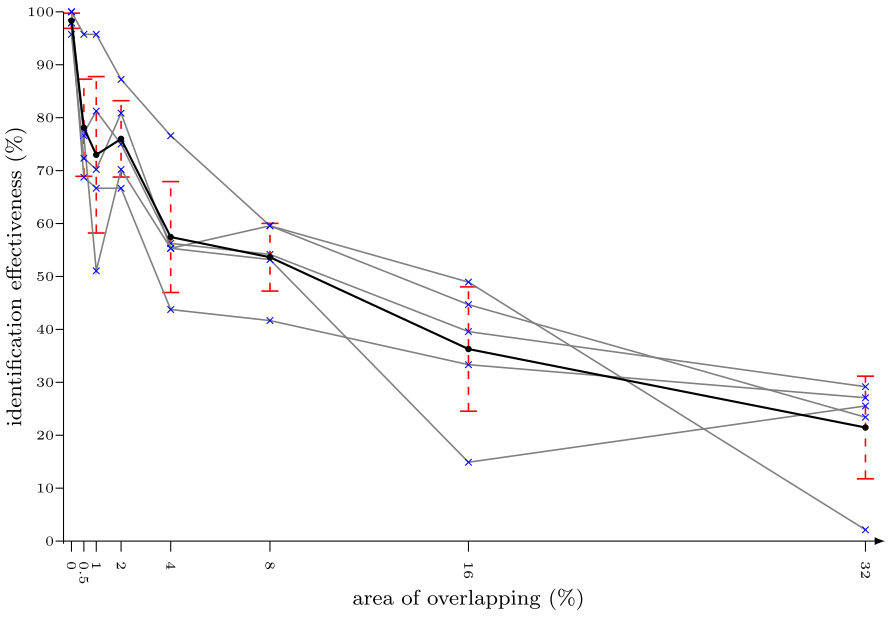

Fig. 11 – Evaluation results using artificial generated scenes (grey lines represent analyses of individual image sets, the thick black line represents the mean value and the vertical red lines depict the standard deviation).

another, and 32% overlapping leads to more or less a green area. These cases can be quite confusing, even for the human brain.

The trend in Fig. 11 shows that generally for low overlapping the algorithm solves the cases nearly to 100%. For moderate overlapping until 5%, every percent of overlay area decreases the identification by 10%. Above 5% overlapping, the scenes are too complex for accurate identification.

Looking at the standard deviation in Fig. 11 it is clear that the effectiveness of the algorithm is also influenced by the randomness of the scene. The reason for this behaviour is because the tests were done only with standard parameters, with no adjustments to the actual situation.

4. Discussion

The pattern recognition method presented here is a new approach to solve an old problem "the plant overlapping problem". It is a simple approach, however it is effective. The results indicate that in situations with low overlapping, the system is able to find the plants with ca. 100% effectiveness. With moderate overlapping the system is still able to give good results. In heavy overlapping the algorithm has not enough information to perform an accurate identification. This, however, was expected because tests with humans using the same artificial images demonstrates that even humans have problems to correctly identify plants with more than 20% overlapping (data not shown). Nevertheless, the evaluation of the algorithm shows that the approach could be used to significantly reduce the overlapping problem in plant science. First applications of the algorithm in the area of weed control prove that last statement (Marx et al., 2012).

Ellipses are powerful shapes, which can cover nearly almost every part of a plant. From round fruits, complex leaves to long small objects (lines) like stems (see Fig. 12).

One of the main advantages of treating leaves as ellipses is the reduction of the complexity of the original leaf shape. But their use allows detection in complex and unknown situations. Therefore, one can conclude that the detection of

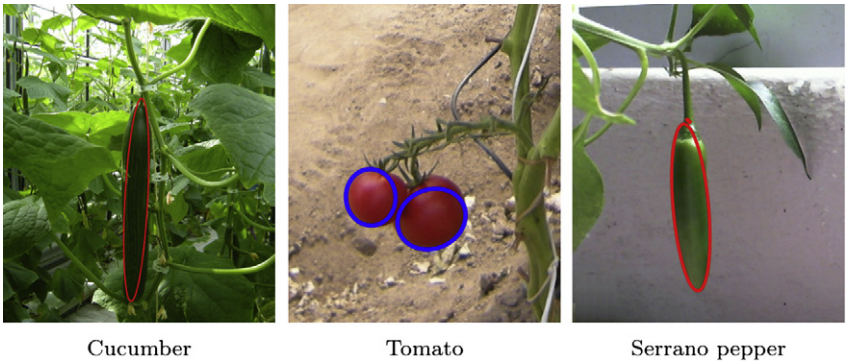

Fig. 12 – Examples of fitting plant shapes with ellipses.

elliptic patterns is an efficient approach to overcome the overlapping problem, because it is possible to calculate and approximate the non-visible part of the objects in an accurate manner. A lot of applications in plant production could directly use this approach to create new and effective automatic machinery: fruit picking systems, apple harvesting robots, flower harvest machines, plant grading systems or weeding machines.

There are several techniques that allow the detection of ellipses, for example, Nguyen, Ahuja, and Wu (2009) and Qiao and Ong (2007). In very complex scenes, the new arc-detection algorithm developed for this work has the advantage that it offers a simple way to locate the arc-sections, which also reduces the computational time of the algorithm. Additionally, one can easily eliminate the small arc-sections by raising the threshold, if it is decided that they are negatively influencing the ellipse detection. Having correct arc-sections is essential before starting the arc combination step; one should remember that in this step the algorithm attempts to merge neighbouring arc-sections with the intention of finding the arcs that belong to the same ellipse. The merging step is also quite straightforward: It is essentially a process that only tries to merge arcs that are interconnected by lines that are fully included in the analysed region. This has the advantage that the algorithm only attempts to merge arcs with high probability of belonging to the same ellipse, thus speeding up the algorithm. Before merging two arcs, there is an ellipse validation step that quantifies the quality of the ellipse produced by the arcs that are being merged. This step prevents the merging of arcs that do not belong to the same ellipse, therefore, maintaining good quality detections.

The fact that additional ellipses might be detected has a direct impact on the following step of plant recognition. This can cause several problems, such as unnecessary combinations with faulty ellipses, faulty plant detections, etc. One might think that unnecessary combinations using the faulty ellipses is to some extent a tolerable error, so long as the correct answer is ultimately found. However, in the case of a very time-sensitive plant identification system, these faulty ellipses will affect its performance, increasing the time to carry out the identification task. The worst case scenario is that the faulty ellipses will lead to the detection of erroneous plants. Certainly, faulty plant detections are an undesirable type of error, because they are detrimental to the overall effectiveness of the plant recognition system.

The proposed leaf detection method works under the assumption that the leaves have to a certain degree an elliptical shape. Naturally, this conjecture was made because it is true that the model plant (tobacco), as well as many other plants species, have leaves in the form of an ellipse. Additionally, this method can also be combined with other techniques which identify non-elliptical leaf shapes. For example, it is possible to think of techniques that fit several ellipses per leaf in order to approximate their shape.

After analysing an image region in the search for leaves, the final step in the plant recognition system is to cluster the detected ellipses into plants. The proposed methodology for carrying out this task is to make decisions using the shape deformation analyses of different ASMs.

There are other researchers who have already put forward systems that use ASMs to identify plants or parts of plants, such as Søgaard and Heisel (2002), who proposed models for the classification of weed plantlets. However, they mention that the classification experiments were carried out without overlapping plants. In spite of this, the identification models were able to classify with an accuracy between 65% and 90%, depending on the weed species. Moeslund, Aagaard, and Lerche (2005) used ASMs to match the shape of cactus leaves before estimating their 3D position. In this case, 86% of the cactus leaves where identified, nevertheless, this is a semi-automatic system where an initial guess of the position and shape of the leaf has to be manually provided for the system to work. Persson and Åstrand (2008), also used ASMs to classify crops and weeds. In this instance, the identification of plants that are partially occluded is also taken into consideration. The suggested procedure is to create deformable models with shape information taken from the non-overlapped plants as well as overlapped plants, where the overlapped plants are treated as a single shape. To some extent, the main idea is to include as many overlapping situations as possible into the system, in order to enable it to identify partly occluded plants. This, of course, can be done up to a certain limit, though one has to be very careful not to over-train the shape model with overlapped shapes. If it is decided to include overlapping situations in the shape model, one has to be aware that the number of possible overlapping situations are infinite, that the shape model is being trained with erroneous shapes, and that there will be a point where the identification will fail because the variance within the training set is too large.

5. Conclusion

The approach proposed in this work uses ASMs as information holders, which only contain information about true plant shapes. No extra information with overlapping plant shapes was supplied to the models. The ability to detect partly occluded plants completely relies on the leaf detection step. In order to find the most probable plants, different combinations of ellipses are landmarked and tested with the ASM: the combinations that are not within the constraints of the model are disregarded, while the combinations that are within the shape constraints are kept for further evaluation.

Summarising, it can be stated that the algorithms described in this work, which are based on ellipse detection and ASMs, are able to overcome in a satisfactory manner the overlapping problem in agriculture. Furthermore, they can be transferred or adapted to other problems because of the very generalised components and structures.

REFERENCES

Brosnan, T., & Sun, D.-W. (2002). Inspection and grading of agricultural and food products by computer vision systems—a review. *Computers and Electronics in Agriculture, 36*, 193–213.

Cheng, H., Jiang, X., Sun, Y., & Wang, J. (2001). Color image segmentation: advances and prospects. *Pattern Recognition, 34*, 2259–2281.

Cootes, T. F., Taylor, C. J., Cooper, D. H., & Graham, J. (1995). Active shape models-their training and application. *Computer Vision and Image Understanding, 61*, 38–59.

Hayashi, S., Shigematsu, K., Yamamoto, S., Kobayashi, K., Kohno, Y., Kamata, J., et al. (2010). Evaluation of a strawberry-harvesting robot in a field test. *Biosystems Engineering, 105*, 160–171.

Hemming, J., & Rath, T. (2001). Computer-vision-based weed identification under field conditions using controlled lighting. *Journal of Agricultural Engineering Research, 78*, 233–243.

Mclaughlin, R. A. (1998). Randomized hough transform: improved ellipse detection with comparison. *Pattern Recognition Letters, 19*, 299–305.

Marx, C., Pastrana, J., Hustedt, M., Barcikowski, S., Haferkamp, H., & Rath, T. (2012). Investigations on the absorption and application of laser radiation for weed control. *Landtechnik, 67*, 95–101.

Moeslund, T. B., Aagaard, M., & Lerche, D. (2005). 3D pose estimation of cactus leaves using an active shape model. In *Proceedings of the seventh IEEE workshops on application of computer vision 2005*, Vol. 1 (pp. 468–473).

Nguyen, T. M., Ahuja, S., & Wu, Q. (2009). A real-time ellipse detection based on edge grouping. In *Systems, Man and Cybernetics, 2009. SMC 2009. IEEE international conference on* (pp. 3280–3286).

Persson, M., & Åstrand, B. (2008). Classification of crops and weeds extracted by active shape models. *Biosystems Engineering, 100*, 484–497.

Qiao, Y., & Ong, S. (2007). Arc-based evaluation and detection of ellipses. *Pattern Recognition, 40*, 1990–2003.

Søgaard, & Heisel (2002). Weed classification by active shape models. In *Automation and emerging technologies – AgEng Budapest, Hungary*.

Suzuki, S., & Abe, K. (1985). Topological structural analysis of digitized binary images by border following. *Computer Vision, Graphics, and Image Processing, 30*, 32–46.

Van Henten, E., Van Tuijl, B., Hemming, J., Kornet, J., Bontsema, J., & Van Os, E. (2003). Field test of an autonomous cucumber picking robot. *Biosystems Engineering, 86*, 305–313.

Woebbecke, D. M., Meyer, G. E., von Bargen, K., & Mortensen, D. A. (1995). Color indices for weed identification under various soil, residue, and lighting conditions. *Transactions of the ASAE, 38*, 259–269.

Yuen, H. K., Illingworth, J., & Kittler, J. (1989). Detecting partially occluded ellipses using the hough transform. *Image Vision Computing, 7*, 31–37.

Zhang, D., & Lu, G. (2004). Review of shape representation and description techniques. *Pattern Recognition, 37*, 1–19.